Mon. Not. R. Astron. Soc. **000**, 000–000 (0000) Printed 28 August 2014 (MN LATEX style file v2.2)

Eccentricity generation in hierarchical triple systems: the planetary regime

Nikolaos Georgakarakos
100 Delphon Str., Thessaloniki 546 43, Greece
email: georgakarakos@hotmail.com

arXiv:1408.6263v1 [astro-ph.EP] 23 Aug 2014

ABSTRACT

In previous papers, we developed a technique for estimating the inner eccentricity in hierarchical triple systems, with the inner orbit being initially circular. We considered systems with well separated components and different initial setups (e.g. coplanar and non-coplanar orbits). However, the systems we examined had comparable masses. In the present paper, the validity of some of the formulae derived previously is tested by numerically integrating the full equations of motion for systems with smaller mass ratios (from 10^{-3} to 10^{3}, i.e. systems with Jupiter-sized bodies). There is also discussion about HD217107 and its planetary companions.

Key words: Celestial mechanics, planetary systems, binaries:general.

1 INTRODUCTION

A hierarchical triple system consists of a binary system and a third body on a wider orbit. The motion of such a system can be pictured as the motion of two binaries on slowly perturbed Keplerian orbits: the binary itself (inner binary) and the binary which consists of the third body and the centre of mass of the binary (outer binary). Hierarchical triple systems are widely present in the galactic field and in star clusters and studying the dynamical evolution of such systems is a key to understanding a number of issues in astronomy and astrophysics, such as tidal friction and dissipation, mass transfer and mass loss due to a stellar wind, which may result in changes in stellar structure and evolution (for systems with *close* inner binaries, where the separation between the components is comparable to the radii of the bodies). But even in systems with well-separated inner binary components, the perturbation of the third body can have a devastating effect on the triple system as a whole (e.g. disruption of the system).

For most hierarchical triple stars, the period ratio X is of the order of 100 and these systems are probably very stable dynamically. However, there are systems with much smaller period ratios, like the system HD 109648 with $X = 22$ (Jha et al. 2000), the λ Tau system, with $X = 8.3$ (Fekel & Tomkin 1982) and the CH Cyg system with $X = 7.0$ (Hinkle et al. 1993).

In two previous papers (Georgakarakos 2002,2003, hereafter HTS1 and HTS2 respectively), we derived formulae for the inner eccentricity in hierarchical triple systems with coplanar and initially circular inner orbit. However, the formulae were only tested for systems with comparable masses within the range $10:1$ (stellar systems). In the present paper, the testing is extended to systems with masses within the range $1000:1$, i.e. systems with Jupiter-sized bodies.

2 THE ECCENTRICITY FORMULAE

At this point, we would like to remind the reader of the formulae that were derived in HTS1 and HTS2. The formula for the circular outer binary case is (with the addition of two more short period terms, i.e. the next order terms in P_2 and P_3 Legendre polynomials; those terms which were included in HTS2 for greater accuracy and were denoted as P_{22} and P_{32}, can be obtained by setting $e = 0$ in equations (9), (11), (13) and (15) of HTS2):

$$\overline{e_1^2} = \frac{m_3^2}{M^2}\frac{1}{X^4}\left(\frac{43}{4} + \frac{225}{128}m_*^2 X^{\frac{2}{3}} + \frac{365}{9}\frac{1}{X^2} + \frac{8361}{2048}m_*^2\frac{1}{X^{\frac{4}{3}}} + \frac{122}{3}\frac{1}{X}\right) + \frac{15}{8}\frac{m_3}{M}\frac{m_*}{X^{\frac{5}{3}}}\frac{C}{A-B} + 2\left(\frac{C}{A-B}\right)^2 \quad (1)$$

with

© 0000 RAS

$$A=\beta,\quad B=1+\frac{75}{8}\gamma,\quad C=\frac{5}{4}\alpha e_{\rm T},\quad e_{\rm T}=\frac{3}{4}\frac{m_1m_2}{(m_1+m_2)^{\frac{4}{3}}M^{\frac{2}{3}}}\frac{1}{X^{\frac{4}{3}}}.$$

The formula for the eccentric outer binary case is (slightly different from the one in HTS2, as some coefficients have been corrected, see Georgakarakos 2005):

$$\begin{aligned}\overline{e_1^2} &= \frac{m_3^2}{M^2}\frac{1}{X^4(1-e^2)^{\frac{9}{2}}}\left[\frac{43}{8}+\frac{129}{8}e^2+\frac{129}{64}e^4+\frac{1}{(1-e^2)^{\frac{3}{2}}}(\frac{43}{8}+\frac{645}{16}e^2+\frac{1935}{64}e^4+\frac{215}{128}e^6)+\frac{1}{X^2(1-e^2)^3}[\frac{365}{18}+\right.\\
&+\frac{44327}{144}e^2+\frac{119435}{192}e^4+\frac{256105}{1152}e^6+\frac{68335}{9216}e^8+\frac{1}{(1-e^2)^{\frac{3}{2}}}(\frac{365}{18}+\frac{7683}{16}e^2+\frac{28231}{16}e^4+\frac{295715}{192}e^6+\frac{2415}{8}e^8+\\
&+\frac{12901}{2048}e^{10})]+\frac{1}{X(1-e^2)^{\frac{3}{2}}}[\frac{61}{3}+\frac{305}{2}e^2+\frac{915}{8}e^4+\frac{305}{48}e^6+\frac{1}{(1-e^2)^{\frac{3}{2}}}(\frac{61}{3}+\frac{854}{3}e^2+\frac{2135}{4}e^4+\frac{2135}{12}e^6+\\
&+\frac{2135}{384}e^8)]+m_*^2X^{\frac{2}{3}}(1-e^2)[\frac{225}{256}+\frac{3375}{1024}e^2+\frac{7625}{2048}e^4+\frac{29225}{8192}e^6+\frac{48425}{16384}e^8+\frac{825}{2048}e^{10}+\frac{1}{(1-e^2)^{\frac{3}{2}}}(\frac{225}{256}+\\
&+\frac{2925}{1024}e^2+\frac{775}{256}e^4+\frac{2225}{8192}e^6+\frac{25}{512}e^8)]+m_*^2\frac{1}{X^{\frac{4}{3}}(1-e^2)^2}[\frac{8361}{4096}+\frac{125415}{8192}e^2+\frac{376245}{32768}e^4+\frac{41805}{65536}e^6+\\
&\left.+\frac{1}{(1-e^2)^{\frac{3}{2}}}(\frac{8361}{4096}+\frac{58527}{2048}e^2+\frac{877905}{16384}e^4+\frac{292635}{16384}e^6+\frac{292635}{524288}e^8)]\right]+2(\frac{C}{B-A})^2. \qquad (2)\end{aligned}$$

with

$$A=\frac{\beta}{(1-e^2)^2},\quad B=\frac{1}{(1-e^2)^{\frac{3}{2}}}+\frac{25}{8}\gamma\frac{3+2e^2}{(1-e^2)^3}\ \text{ and }\ C=\frac{5}{4}\alpha\frac{e}{(1-e^2)^{\frac{5}{2}}}.$$

In both cases:

$$\alpha=\frac{m_1-m_2}{m_1+m_2}\frac{a_1}{a_2},\quad \beta=\frac{m_1m_2M^{\frac{1}{2}}}{m_3(m_1+m_2)^{\frac{3}{2}}}(\frac{a_1}{a_2})^{\frac{1}{2}},\quad \gamma=\frac{m_3}{M^{\frac{1}{2}}(m_1+m_2)^{\frac{1}{2}}}(\frac{a_1}{a_2})^{\frac{3}{2}},$$

e is the outer eccentricity and a_1 and a_2 are the inner and outer semi major axes respectively. Also, M is the total mass of the system, $m_*=\frac{m_2-m_1}{(m_1+m_2)^{\frac{2}{3}}M^{\frac{1}{3}}}$ and X is the period ratio of the two orbits.

3 NUMERICAL TESTING

In order to test the validity of the formulae derived in the previous papers, we integrated the full equations of motion numerically, using a symplectic integrator with time transformation (Mikkola 1997).

The code calculates the relative position and velocity vectors of the two binaries at every time step. Then, by using standard two body formulae, we computed the orbital elements of the two binaries. The various parameters used by the code, were given the following values: writing index $Iwr=1$, method coefficients $a1=1$ and $a2=15$, correction index $icor=1$. The average number of steps per inner binary period NS, was given the value of 60 for testing the short period terms and the long term circular case. For the long period eccentric cases, we set $NS=5$ in order to accelerate the execution of the code, without any precision cost, as the motion was mainly dominated by secular evolution.

For our simulations, we also defined the two mass ratios

$$K1=\frac{m_1}{m_1+m_2}\ \text{ and }\ K2=\frac{m_3}{m_1+m_2},$$

with $0.001\leq K1\leq 0.5$ and $0.001\leq K2\leq 1000$.

Following HTS2, for the eccentric outer binary case, we used the fictitious initial period ratio X_{0f}, defined as the ratio of the period that the outer binary would have on a circular orbit with a semi major axis equal to its periastron distance over the period of the inner binary. In all cases $X_{0f}\geq 10$. We also used units such that $G=1$ and $m_1+m_2=1$ and we always started the integrations with $a_1=1$. In that system of units, the initial conditions for the numerical integrations were as follows:

$$r_1=1,\qquad r_2=0,\qquad r_3=0$$

$$R_1=a_2\cos\phi,\qquad R_2=a_2\sin\phi,\qquad R_3=0$$

$$\dot{r}_1=0,\qquad \dot{r}_2=1,\qquad \dot{r}_3=0$$

$$\dot{R}_1=-\sqrt{\frac{M}{a_2}}\sin\phi,\qquad \dot{R}_2=\sqrt{\frac{M}{a_2}}\cos\phi,\qquad \dot{R}_3=0,$$

for the circular case (ϕ is the initial relative phase of the two binaries) and

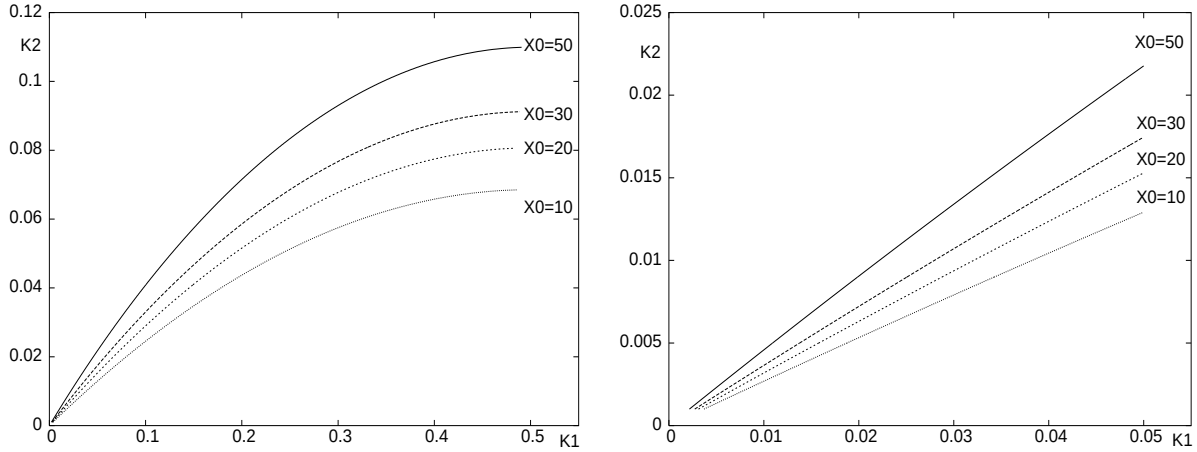

Figure 1. $K2$ against $K1$ for $e = 0$ and for which $A - B = 0$. The right graph is the same as the left one, but for $K1 \leq 0.05$.

$r_1 = 1, \quad r_2 = 0, \quad r_3 = 0$

$R_1 = R_0 \cos(f_0 + \varpi), \quad R_2 = R_0 \sin(f_0 + \varpi), \quad R_3 = 0$

$\dot{r}_1 = 0, \quad \dot{r}_2 = 1, \quad \dot{r}_3 = 0$

$$\dot{R}_1 = -\sqrt{\frac{M}{a_2(1-e^2)}} \sin(f_0 + \varpi), \quad \dot{R}_2 = \sqrt{\frac{M}{a_2(1-e^2)}} \cos(f_0 + \varpi), \quad \dot{R}_3 = 0.$$

for the non circular case, where f_0 and ϖ are the initial true anomaly and longitude of pericentre respectively of the outer orbit.

3.1 LONG PERIOD EVOLUTION

First, we present the results from testing equations (1) and (2) for long term behaviour. The formulae were compared with results obtained from integrating the full equations of motion numerically.

For the circular case, each system was numerically integrated for $\phi = 0^\circ - 360^\circ$ with a step of 45°. After each run, $e_{\rm in}^2$ was averaged over time using the trapezium rule and after the integrations for all ϕ were done, we averaged over ϕ by using the rectangle rule. The integrations were also done for smaller steps in ϕ (e.g. 1°), but was not any difference in the outcome.

For the non circular case, each system was numerically integrated for $\varpi = 0^\circ - 360^\circ$ and $f_0 = 0^\circ - 360^\circ$ with a step of 60°. For a given value of ϖ and f_0 we integrated our system. After each run, $e_{\rm in}^2$ was averaged over time using the trapezium rule and then we integrated the system for a different f_0. After the integrations for all f_0 were done, we averaged over f_0 by using the rectangle rule. Then, the same procedure was applied for the next value of ϖ and when the integrations for all ϖ were done, we averaged over ϖ by using the rectangle rule. The integrations were also done for smaller steps in ϖ and f_0, but the difference in the outcome was insignificant.

These results are presented in Tables 1, 2 and 3 ($e = 0, 0.4, 0.75$ respectively), which give the percentage error between the averaged numerical $e_{\rm in}^2$ and equations (1) and (2). The error is accompanied by the period of the oscillation of the eccentricity, which is the same as the integration time span (when there is no period given, we integrated for an outer orbital period, i.e $2\pi X$, as there was not any noticeable secular evolution). There are four values per $(K1 - K2)$ pair, corresponding, from top to bottom, to $X = 10, 20, 30, 50$ respectively (of course, for the eccentric outer binary case, X is replaced by X_{0f}).

Generally, it appears that the theory is in agreement with the numerical integrations. There are some cases (larger $K2$) where the error is rather significant (around 30%; however, the reader should have in mind that the error is in e^2, which means that it is about double than the one in e), but it dropped as the period ratio increased. There are also some cases where the formulae do not seem to work well; in fact, for some systems (e.g. $e = 0.75$, $K1 = 0.005$,$K2 = 0.001$) we have a complete failure of our formula. For those cases, our formula gives an overestimate of the inner eccentricity (our secular solution has larger period and amplitude of oscillation) and that is due to the fact that $A - B$ gets small, i.e. our approximate secular solution is near resonance. This is demonstrated in figures 1,2 and 3, which are plots of $K2$ against $K1$ for which $A - B = 0$. Finally, for large eccentricities, there is a significant error for $K1 = 0.5$ and $X_{0f} = 10$, which is due to terms omitted from the approximate secular solution. Those terms become insignificant as X_{0f} increases.

Table 1. Percentage error between the averaged numerical e_1^2 and equation (1). For all systems, $e = 0$.

$K2\backslash\ K1$	0.001	0.005	0.01	0.05	0.1	0.5
0.001	-4.5 (1.1510^6)	-3 (4.710^5)	6.9 (210^5)	9.4 (3.510^4)	9.7 (1.910^4)	12.2
	-1.5 (510^6)	-15.7 (3.510^6)	2.3 (1.110^6)	3 (1.910^5)	3.1 (10^5)	3.7
	0.4 (1.0510^7)	-16.8 (1.0510^7)	2.4 (310^6)	1.7 (510^5)	1.7 (2.610^5)	1.9
	-1.2 (310^7)	-29.4 (510^7)	-0.4 (1210^6)	0.9 (1.710^6)	0.9 (8.510^5)	0.8
0.01	10.2	8.3 (10^5)	-4 (1.210^5)	-1.7 (5.310^4)	8.3(2.310^4)	12.2
	2.1	3.9 (3.610^5)	-0.9 (510^5)	-15.9 (410^5)	2.8 (1.310^5)	3.8
	0.3	2.7 (810^5)	-0.5 (1.110^6)	-17 (1.210^6)	1.6 (3.710^5)	1.9
	-0.8	0.5 (2.510^6)	0.7 (2.810^6)	-37 (6.110^6)	-2.2 (1.510^6)	0.8
0.1	13.8	13.3	12.6	11.4 (910^3)	7 (1.110^4)	12.8
	5.4	4.7	5.1 (3.510^4)	4.6 (410^4)	2.8 (510^4)	4
	3.3	2.5	3 (910^4)	3.1 (910^4)	2.2 (1.110^5)	2.1
	1.8	1	1.8 (2.210^5)	1.9 (2.510^5)	1.2 (310^5)	1
1	26.7	26.6	26.4	25	23.5	17.3
	12.8	12.7	12.6	11.5	10.2	5.9
	8.8	8.7	8.6	7.6	6.8 (1.510^4)	3.2
	5.6	5.5	5.4	4.5	4.3 (4.510^4)	1.6
10	36	35.9	35.7	34.5	32.9	26.2
	14.7	14.7	14.6	13.8	12.8	8.4
	9.8	9.7	9.6	8.9	8.2	4.6
	6.2	6.2	6.1	5.6	5.4	2.2
100	31.4	31.4	31.4	30.9	30.4	28.3
	10.9	10.8	10.8	10.5	10.2	8.9
	6.5	6.4	6.4	6.2	5.9	4.8
	3.7	3.7	3.6	3.5	3.2	2.3
1000	29.3	29.4	29.2	29.1	29	28.5
	9.4	9.4	9.4	9.3	9.2	8.9
	5.2	5.2	5.2	5.2	5.1	4.8
	2.7	2.7	2.7	2.6	2.6	2.4

3.2 SHORT PERIOD EVOLUTION

In order to be consistent with papers HTS1 and HTS2, and for completeness reasons, we also present results from comparing the numerical and theoretical inner eccentricity, on shorter timescales. The results, presented in Tables 4,5 and 6, show the percentage error between the averaged numerical and theoretical inner eccentricity (equations (30) and (31) of HTS1 with the modification mentioned in section 2 and equations (28) and (29) of HTS2). Again, there are four entries per $(K1 - K2)$ pair, corresponding, from top to bottom, to $X = 10, 20, 30, 50$ respectively. The integrations were done with $\phi = 90^\circ$ for a circular outer binary and with $f_0 = 90^\circ$ and $\varpi = 0^\circ$ for a system with an eccentric outer binary. However, this does not affect the qualitative understanding of the problem at all; similar results are obtained for different initial conditions and an example of that is given in Table 7.

4 APPLICATIONS IN EXOSOLAR PLANETARY SYSTEMS: THE HD217107 SYSTEM

In the past decade, 155 planets have been discovered orbiting stars other than our Sun, with properties that are somehow different compared to our solar system (e.g. eccentric orbits are rather common among exoplanets). Among them, multiple planetary systems have been detected around 17 stars, by use of the Doppler technique. For a summary of those developments up to date, see Marcy et al. 2005. Here, we discuss some possible applications of our formula on exoplanets, although that was not our initial intention when we started this work, firstly presented in HTS1.

From the multiple exoplanetary systems that have been discovered so far, we picked up HD217107, which has a dynamical setup similar to the one we study in our paper (well separated components, no mean motion commensurabilities). So far, two planets have been detected orbiting HD217107 (Fischer et al. 1999, 2001; Vogt et al. 2005). The orbital elements of the system are given in Table 8.

Table 2. Percentage error between the averaged numerical e_1^2 and equation (2). For all systems, $e = 0.4$.

$K2\backslash\ K1$	0.001	0.005	0.01	0.05	0.1	0.5
0.001	-8.5 (4.7310^6)	-35.8 (2.510^6)	-8.1 (9.510^5)	-0.9 (1.6110^5)	0.2 (8.310^4)	12.9 (1.510^4)
	-2.8 (1.7210^7)	-40.6 (1.810^7)	-4.9 (5.510^6)	-0.6 (8.5110^5)	-0.1 (4.3510^5)	3.8 (810^4)
	-2 (3.710^7)	-55.5 (6.0410^7)	-3.7 (1.5410^7)	-0.3 (2.2310^6)	-0.2 (1.13510^6)	2 (210^5)
	-0.9 (9.710^7)	-171.6 (3.1310^8)	-2.8 (5.7510^7)	-0.2 (7.510^6)	-0.2 (3.7910^6)	1.1 (6.6510^5)
0.01	0.4 (310^5)	-2.6 (3.610^5)	-7.8 (4.710^5)	-36.3 (2.8610^5)	-5.1 (1.1110^5)	12.9(1.810^4)
	-0.3 (1.2310^6)	-0.3 (1.410^6)	-1.7 (1.7110^6)	-42.4 (2.0610^6)	-3.5 (6.4510^5)	3.8 (8.510^4)
	-0.1 (2.7710^6)	-0.6 (3.1210^6)	-0.9 (3.6810^6)	-65.5 (7.0710^6)	-2.8 (1.8210^6)	2.2 (2.310^5)
	-0.2 (7.710^6)	-0.4 (8.510^6)	-0.7 (9.7510^6)	-333.2 (3.8210^7)	-2.7 (6.9410^6)	1.6 (7.9510^5)
0.1	-0.6 (310^4)	-1 (3.0510^4)	-0.4 (3.0810^4)	-2.6 (3.610^4)	-5.5 (4.4510^4)	14.6 (1.910^5)
	1.6 (1.2610^5)	1.6 (1.27510^5)	1.1 (1.310^5)	0.4 (1.4810^5)	-0.4 (1.7510^5)	6.8 (2.710^5)
	1.4 (2.8810^5)	1 (2.9210^5)	1 (2.9610^5)	1.1 (3.310^5)	0.3 (3.8310^5)	3.6 (4.610^5)
	0.9 (8.110^5)	0.6 (8.210^5)	0.5 (8.310^5)	0.6 (9.110^5)	0.5 (1.02510^6)	1.7 (9.810^5)
1	1.4 (4.210^3)	4.2 (4.0510^3)	5.4 (410^3)	3.5 (4.110^3)	4 (4.110^5)	17.7 (2.410^3)
	8 (210^4)	7.9 (210^4)	7.1 (2.0210^4)	9 (210^4)	7.9 (2.0510^4)	5.6 (1.110^4)
	6.3 (4.810^4)	6.4 (4.810^4)	6.5 (4.810^4)	7.5 (4.810^4)	6.8 (4.910^4)	3.2 (2.710^4)
	4.2 (1.410^5)	4.3 (1.410^5)	4.4 (1.410^5)	4 (1.4210^5)	4.4 (1.4310^5)	2 (7.510^4)
10	16.8 (3.910^4)	16.5 (410^4)	16.6 (410^4)	17 (410^4)	17 (410^4)	24.3 (4.410^3)
	12.4 (10^4)	14.6 (9.710^3)	16.3 (9.510^3)	14.7 (9.710^3)	13.1 (9.910^3)	8 (510^3)
	10.9 (2.4510^4)	12.5 (2.410^4)	10.4 (2.4610^4)	10.9 (2.4510^4)	12.8 (2.410^4)	4.7 (1.310^4)
	8.1 (7.310^4)	0.2 (7.310^4)	8.1 (7.310^4)	8.2 (7.310^4)	8.4 (7.310^4)	2.7 (3.810^4)
100	21.5 (1.610^3)	20.7 (1.610^3)	20.8 (1.610^3)	21.3 (1.610^3)	21.9 (1.610^3)	27.1
	13 (910^3)	12.5 (910^3)	12.5 (910^3)	14.1 (8.810^3)	9.3 (9.410^3)	8.4 (510^3)
	8.5 (2.310^4)	12 (2.210^4)	12 (2.210^4)	12 (2.210^4)	12 (2.210^4)	5 (1.110^4)
	9.3 (6.610^4)	7.8 (6.710^4)	7.8 (6.710^4)	7.9 (6.710^4)	7.8 (6.710^4)	2.8 (3.410^4)
1000	24.5 (1.610^3)	24 (1.610^3)	24 (1.610^3)	24.2 (1.610^3)	24.5 (1.610^3)	27.1
	11 (910^3)	13.7 (8.510^3)	13.6 (8.510^3)	12.7 (8.610^3)	10.7 (8.910^3)	8.3 (4.810^3)
	9 (2.2510^4)	13.9 (2.110^4)	12.2 (2.1510^4)	13.6 (2.110^4)	10.1 (2.210^4)	4.8 (1.0510^4)
	9.6 (6.510^4)	8.2 (6.610^4)	8.2 (6.610^4)	8.2 (6.610^4)	9.4 (6.510^4)	2.7 (3.310^4)

Assuming that the two binaries move in coplanar orbits and substituting the HD217107 orbital elements into formula (2), we get that $\sqrt{\overline{e_1^2}} \approx 0.025$ (Keck) and $\sqrt{\overline{e_1^2}} \approx 0.028$ (Lick) (with $\sin i = 1$, i being the inclination of the orbital plane with the plane of the sky). Fig. 4 is a plot of inner eccentricity against time for a system with the orbital parameters of HD217107 and it is obtained by integrating the full equations of motion numerically using our symplectic code ($e_{10} = 0$, $f_0 = 0^\circ$, $\varpi = 0^\circ$). As one can see, the maximum eccentricity is around 0.04, a value that is much smaller than the observed one of around 0.13 (our theoretical model produces the same graphs). We would probably be able to have an orbit with a larger eccentricity if we started the system with a small but non zero eccentricity, e.g. 0.08 would give us a maximum eccentricity around 0.13. However, this may not be a good assumption to make, as the planet is very close to the star ($a = 0.074AU$) and tidal circularisation would be expected to take place. Therefore, we would still need a not so small perturbation to the inner orbit, capable of maintaining an eccentricity of at least 0.13 (we say at least, because we do not really know which phase of the eccentricity oscillation we currently see). We also performed integrations varying $\sin i$, but with very little effect on the eccentricity. What seemed to affect things, was to consider a system with a larger outer eccentricity (for example, for $e_{\rm out} = 0.8$, the maximum $e_{\rm in}$ was around 0.12).

Another possibility of course, is that the two orbits are not coplanar. In the case of low mutual inclination I ($I < 39.23^\circ$ or $I > 140.77^\circ$), our past experience from circular binaries (Georgakarakos 2004) and some quick numerical integrations of the secular equations of motion with a 4th-order Runge-Kutta method with variable stepsize (Press et al. 1996; for the secular equations see Marchal 1990), led us to the conclusion that there was little difference between the eccentricity of a coplanar and a non coplanar orbit, with the rest of the orbital elements being the same (an exception here might be the occurence of a secular resonance between the two pericentre frequencies, which can increase the amplitude of the eccentricity oscillation). On the other hand, in the case of high mutual inclination ($39.23^\circ < I < 140.77^\circ$), it is known that the eccentricity can reach significant values, it can even become one for $I = 90^\circ$ ($e_{\max} = \sqrt{1 - \frac{5}{3}\cos^2 I}$; more about the high and low inclination regimes in Kozai 1962).

Table 3. Percentage error between the averaged numerical e_1^2 and equation (2). For all systems, $e = 0.75$.

$K2\backslash\ K1$	0.001	0.005	0.01	0.05	0.1	0.5
0.001	6.8 (2.6410^7)	-54.8 (1.6110^7)	-10.8 (5.8210^6)	-2.6 (9.510^5)	-0.8 (4.8810^5)	81.8 (8.510^4)
	1.3 (8.810^7)	-84.9 (1.1610^8)	-5.9 (3.410^7)	-0.5 (510^6)	0.1 (2.5410^6)	5.6 (4.310^5)
	0.3 (1.8710^8)	-176.2 (3.9110^8)	-4.6 (9.610^7)	-0.2 (1.3110^7)	-0.2 (6.6410^6)	2.6 (1.110^6)
	0.3 (4.910^8)	-8233.2 (1.9210^9)	-4.2 (3.6710^8)	-0.3 (4.4210^7)	-0.1 (2.21510^7)	1.1 (3.810^6)
0.01	3.6 (1.6310^6)	4 (1.9310^6)	6.6 (2.610^6)	-55.7 (1.8110^6)	-7.4 (6.7710^5)	70 (910^4)
	0.5 (6.4510^6)	0.8 (7.310^6)	1.4 (8.810^6)	-100.5 (1.3310^7)	-4.3 (410^6)	5.5 (510^5)
	0.7 (1.4410^7)	0.3 (1.6110^7)	0.7 (1.8710^7)	-262.9 (4.5510^7)	-3.8 (1.14710^7)	2.7 (1.410^6)
	0.1 (410^7)	0.3 (4.3610^7)	0.1 (4.9410^7)	-4855 (2.2810^8)	-3.8 (4.4910^7)	1.2 (4.610^6)
0.1	1.8 (1.6110^5)	2.1 (1.6310^5)	2.1 (1.6610^5)	1.8 (1.9310^5)	1.7 (2.3710^5)	37.8 (3.310^5)
	1.3 (6.6510^5)	0.9 (6.7510^5)	1.1 (6.8310^5)	1.3 (7.6510^5)	0.9 (8.9210^5)	5.7 (10^6)
	0.8 (1.51510^6)	1.1 (1.52510^6)	0.7 (1.5510^6)	0.9 (1.7110^6)	0.9 (1.9410^6)	2.8 (210^6)
	0.4 (4.2410^6)	0.6 (4.2710^6)	0.5 (4.3210^6)	0.4 (4.710^6)	0.5 (5.2110^6)	1.3 (4.410^6)
1	-3.4 (2.210^4)	-3.3 (2.210^4)	-3.3 (2.210^4)	-5.5 (2.2510^4)	-5.5 (2.2510^4)	36.7 (1.1410^4)
	2.6 (1.0810^5)	3.6 (1.0710^5)	4.6 (1.0610^5)	2.6 (1.0910^5)	2.6 (1.110^5)	7.1 (5.810^4)
	3.1 (2.5510^5)	3.6 (2.5410^5)	3.7 (2.5410^5)	3.8 (2.5610^5)	3.2 (2.610^5)	3.7 (1.410^5)
	2.5 (7.3510^5)	2.6 (7.3510^5)	2.3 (7.3810^5)	2.9 (7.410^5)	2.5 (7.510^5)	2.1 (3.910^5)
10	2.7 (910^3)	-6.3 (10^4)	-7 (10^4)	-2.6 (9.510^3)	3.2 (910^3)	35 (4.510^3)
	8.3 (5.110^4)	6.6 (5.210^4)	6.6 (5.210^4)	6.6 (5.210^4)	6.6 (5.210^4)	9.4 (2.710^4)
	7 (1.2810^5)	5.6 (1.310^5)	5.6 (1.310^5)	6.4 (1.2910^5)	6.5 (1.2910^5)	5.2 (610^4)
	4.8 (3.8510^5)	4.8 (3.8510^5)	4.8 (3.8510^5)	4.2 (3.8810^5)	4.1 (3.8910^5)	2.7 (210^5)
100	11 (8.510^3)	10.8 (8.510^3)	10.9 (8.510^3)	12.2 (8.510^3)	16.4 (8.510^3)	31.8 (410^3)
	6.3 (4.710^4)	4.4 (4.810^4)	4.4 (4.810^4)	6.3 (4.710^4)	2.7 (4.910^4)	10 (2.510^4)
	6.4 (1.1710^5)	7.2 (1.1610^5)	7.2 (1.1610^5)	6.4 (1.1710^5)	5.7 (1.1810^5)	5.8 (5.810^4)
	5.3 (3.510^5)	5.3 (3.510^5)	5.3 (3.510^5)	5.3 (3.510^5)	5.3 (3.510^5)	3 (1.7510^5)
1000	33.5 (810^3)	33.6 (810^3)	33.8 (810^3)	35.3 (810^3)	37 (810^3)	38.8 (410^3)
	4.1 (4.810^4)	4.1 (4.810^4)	4.1 (4.810^4)	4.3 (4.810^4)	4.6 (4.810^4)	10 (2.510^4)
	6.2 (1.1610^5)	7 (1.1510^5)	7 (1.1510^5)	7 (1.1510^5)	7 (1.1510^5)	5.7 (5.810^4)
	4.9 (3.4810^5)	4.9 (3.4810^5)	4.9 (3.4810^5)	4.9 (3.4810^5)	4.9 (3.4810^5)	3 (1.7510^5)

Thus, as a conclusion, we could say that with the current information about the HD217107 system, the planets that have been detected there so far is not very likely to move on the same plane. Unfortunately, the two formulae presented in this paper (eqns. (1) and (2)) are only applicable for hierarchical triple systems on coplanar orbits (or orbits with a mutual inclination of a few degrees) and hence, they can not be used to place further constraints to the system.

We would like to point out here that equations (1) and (2) are purely classical and do not take into account any relativistic effects. However, in situations where a planet is very close to the host star, relativistic apsidal precession of the inner orbit could affect the evolution of eccentricity (e.g. see Holman et al. 1997, Ford et al. 2000, Mardling & Lin 2002).

5 SUMMARY

In two previous papers, we derived formulae for estimating the inner eccentricity in hierarchical triple systems with coplanar orbits and with the inner eccentricity being initially zero. However, those calculations were done for systems with comparable masses. In the present paper, we tested the formulae for systems with mass ratios from 10^{-3} to 10^3. The theoretical models appeared to work well for most of the cases. There were a few cases for which the theory did not work well, but no theory is perfect. Finally, we applied the theory on the exosolar planetary system HD217107, in an attempt to obtain more information about its orbital characteristics, although that kind of application was not part of the initial motivation for the construction of the models. We concluded that the two planets orbiting the host star are probably on non coplanar orbits. The derivation of a three dimensional formula for eccentric binaries is one of our future aims, as it would definitely prove more helpful for various dynamical problems, especially with the constant discovery of more and more exosolar planets every day.

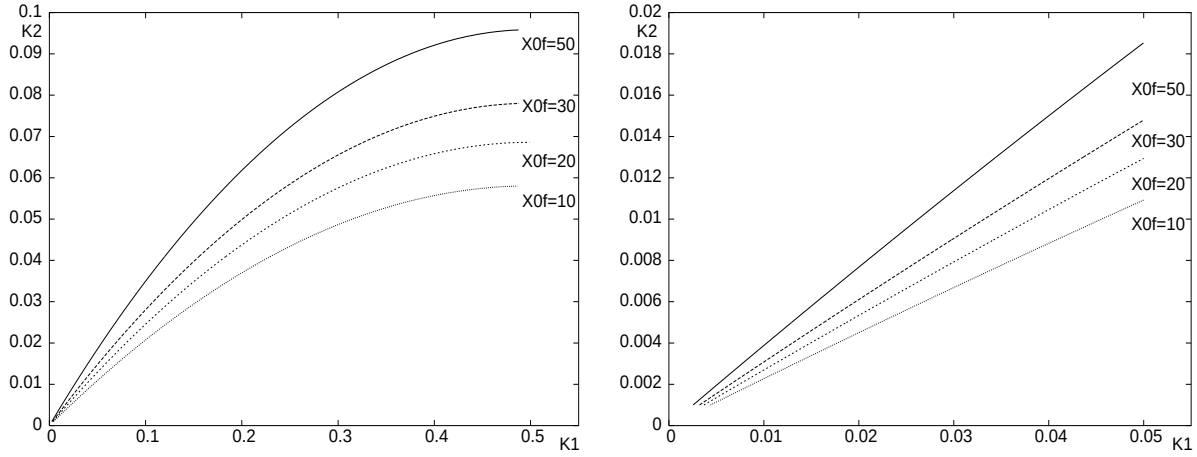

Figure 2. $K2$ against $K1$ for $e = 0.4$ and for which $A - B = 0$. The right graph is the same as the left one, but for $K1 \leq 0.05$.

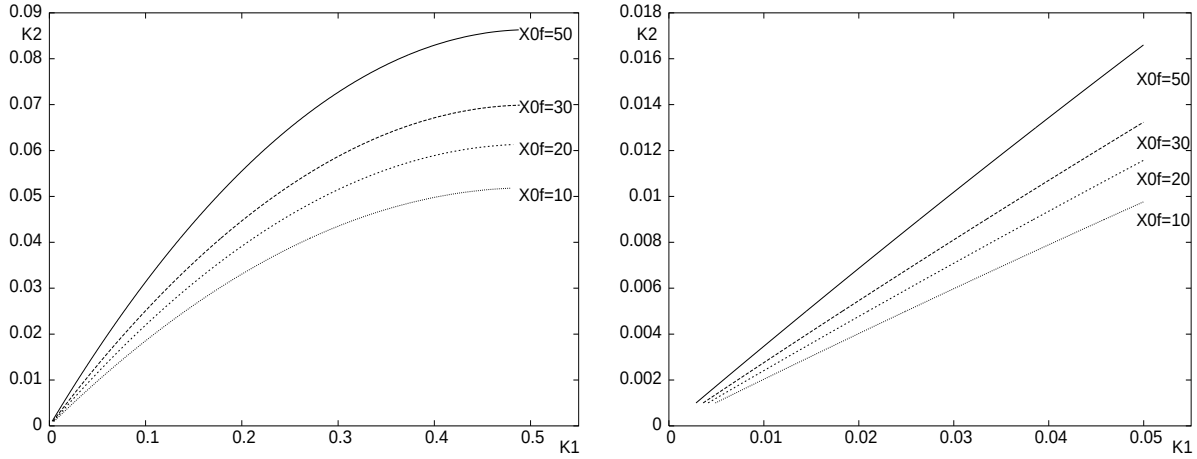

Figure 3. $K2$ against $K1$ for $e = 0.75$ and for which $A - B = 0$. The right graph is the same as the left one, but for $K1 \leq 0.05$.

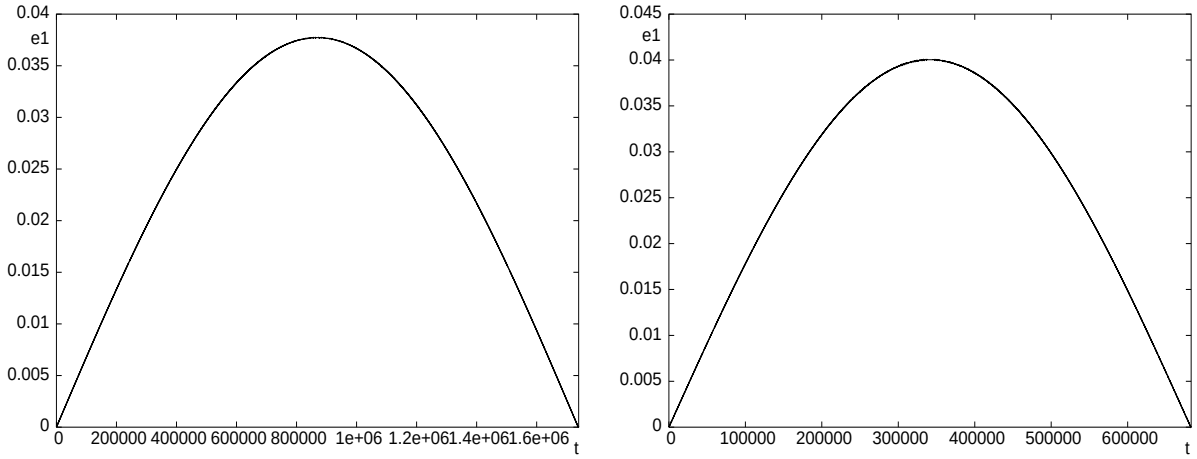

Figure 4. Inner eccentricity against time for HD217107. The graphs come from the numerical integration of the full equations of motion (the left graph is based on the Keck Observatory data, while the left one uses data from Lick Observatory). The initial conditions are $e_{10} = 0$, $f_0 = 0^\circ$ and $\varpi = 0^\circ$. The time t is in yrs (the period of oscillation for the left graph is 1.7410^6 yrs and 6.8310^5 yrs for the right one).

Table 4. Percentage error between the averaged numerical and averaged theoretical e_1. The theoretical model is based on equations (30) and (31) of HTS1. For all systems, $e = 0$ and $\phi = 90°$.

$K2\backslash K1$	0.001	0.005	0.01	0.05	0.1	0.5
0.001	4.9	4.7	5	5.1	5.3	5.2
	1.6	1.6	1.6	1.6	1.7	1.4
	0.9	0.9	0.9	0.9	0.9	0.6
	0.4	0.4	0.4	0.4	0.4	0.3
0.01	5.2	5.2	5.2	5.3	5.5	5.4
	1.7	1.7	1.7	1.7	1.7	1.4
	0.9	0.9	0.9	0.9	0.9	0.7
	0.5	0.5	0.5	0.5	0.5	0.3
0.1	7.1	7.1	7.1	7.2	7.3	7.1
	2.6	2.6	2.6	2.6	2.6	2.2
	1.6	1.6	1.6	1.5	1.5	1.1
	0.9	0.9	0.9	0.8	0.8	0.5
1	17.6	17.6	17.6	17.5	17.2	16
	7.3	7.2	7.2	7.1	6.9	5.9
	4.6	4.6	4.6	4.5	4.3	3.4
	2.7	2.7	2.7	2.6	2.5	1.8
10	27.7	27.7	27.6	27.4	27.2	26.4
	11	11	11	10.9	10.7	9.9
	6.8	6.7	6.7	6.6	6.5	5.8
	3.8	3.8	3.8	3.7	3.6	3.1
100	28.5	28.5	28.5	28.5	28.4	28.4
	11.1	11.1	11.1	11	11	10.8
	6.6	6.6	6.6	6.5	6.5	6.3
	3.6	3.6	3.6	3.6	3.5	3.4
1000	28.5	28.5	28.5	28.5	28.5	28.6
	10.9	10.9	10.9	10.9	10.9	10.8
	6.4	6.4	6.4	6.4	6.4	6.4
	3.5	3.5	3.5	3.5	3.4	3.4

ACKNOWLEDGMENTS

The author wants to thank Douglas Heggie for the useful discussion concerning this paper and Seppo Mikkola, who kindly provided the code for integrating hierarchical triple systems.

REFERENCES

Fekel F. C., Jr., Tomkin J., 1982, ApJ 263, 289
Fischer D. A., Marcy G. W., Butler R. P., Vogt S. S., Apps K., 1999, PASP, 111, 50
Fischer D. A., Marcy G. W., Butler R. P., Vogt S. S., Frink S., Apps K., 2001, ApJ, 551, 1107
Ford E. B., Kozinsky B., Rasio F. A., 2000, ApJ, 535, 385
Georgakarakos N., 2002, MNRAS, 337, 559
Georgakarakos N., 2003, MNRAS, 345, 340
Georgakarakos N., 2004, CeMDA, 89, 63
Georgakarakos N., 2005, MNRAS, 362, 748
Hinkle K. H., Fekel F. C., Johnson D. S., Scharlach W. W. G., 1993, AJ, 105, 1074
Jha S., Torres G., Stefanik R. P., Latham D. W., Mazeh T., 2000, MNRAS, 317, 375
Holman M., Touma J., Tremaine S.,1997, Nat, 386, 254
Kozai Y., 1962, AJ, 67, 591
Marchal C., 1990, The Three-Body Problem. Elsevier Science Publishers, the Netherlands
Marcy G. W., Butler R. P., Fischer D. A., Vogt S. S., Wright J. T., Tinney C. G., Jones H. R. A., 2005, PThPS, 158, 24

Table 5. Percentage error between the averaged numerical and averaged theoretical e_1. The theoretical model is based on equations (28) and (29) of HTS2. For all systems, $e = 0.4$, $f_0 = 90^\circ$ and $\varpi = 0^\circ$.

$K2\backslash\ K1$	0.001	0.005	0.01	0.05	0.1	0.5
0.001	2.5	2.5	2.5	2.5	2.5	2.2
	0.8	0.8	0.8	0.8	0.7	0.6
	0.4	0.4	0.4	0.4	0.4	0.3
	0.2	0.2	0.2	0.2	0.2	0.1
0.01	2.7	2.7	2.7	2.6	2.6	2.3
	0.9	0.9	0.8	0.8	0.8	0.6
	0.5	0.5	0.5	0.5	0.4	0.3
	0.2	0.2	0.2	0.2	0.2	0.1
0.1	3.8	3.7	3.7	3.7	3.6	2.9
	1.5	1.5	1.5	1.4	1.4	1
	1	1	1	0.9	0.9	0.5
	0.6	0.6	0.6	0.5	0.5	0.2
1	9.1	9.1	9	8.7	8.4	6.3
	4.5	4.5	4.5	4.3	4	2.7
	3.1	3.1	3	2.9	2.7	1.5
	2	2	2	1.9	1.7	0.9
10	12.8	12.8	12.7	12.5	12.1	10.4
	5.9	5.9	5.9	5.7	5.5	4.5
	3.8	3.8	3.8	3.7	3.5	2.6
	2.4	2.4	2.4	2.3	2.2	1.5
100	12.1	12.1	12.1	12	11.9	11.2
	5.3	5.3	5.3	5.2	5.2	4.9
	3.2	3.2	3.2	3.2	3.1	2.8
	1.9	1.9	1.9	1.9	1.8	1.6
1000	11.7	11.7	11.6	11.6	11.6	11.3
	5	5	5	5	5	4.9
	3	3	3	3	2.9	2.8
	1.7	1.7	1.7	1.7	1.7	1.6

Mardling R.A., Lin D.N.C., 2002, ApJ, 573, 829
Mikkola S., 1997, CeMDA, 67, 145
Press W. H., Teukolsky S. A., Vetterling W. T., Flannery B. P., 1996, Numerical Recipes In Fortran 77 (2nd ed.). Cambridge Univ. Press, NY
Vogt S. S., Butler R. P, Marcy G. W., Fischer D. A., Henry G. W., Laughlin G., Wright J. T., Johnson J. A., 2005, ApJ, 632, 638

Table 6. Percentage error between the averaged numerical and averaged theoretical e_1. The theoretical model is based on equations (28) and (29) of HTS2. For all systems, $e = 0.75$, $f_0 = 90^\circ$ and $\varpi = 0^\circ$.

$K2\backslash\ K1$	0.001	0.005	0.01	0.05	0.1	0.5
0.001	-0.1	-0.1	-0.1	0.2	0.6	0.5
	-0.7	-0.6	-0.6	-0.4	-0.2	0.1
	-1.2	-1.2	-1.2	-0.9	-0.6	0.1
	-2	-1.9	-1.9	-1.6	-1.2	0.1
0.01	-0.1	-0.1	0.1	0.2	0.7	0.6
	-0.6	-0.6	-0.6	-0.4	-0.1	0.1
	-1.2	-1.2	-1.1	-0.9	-0.6	0.1
	-1.9	-1.9	-1.9	-1.6	-1.2	0.1
0.1	0.4	0.4	0.4	0.7	1.1	1.1
	-0.3	-0.3	-0.3	-0.1	0.1	0.4
	-0.9	-0.9	-0.9	-0.6	-0.4	0.2
	-1.7	-1.7	-1.6	-1.3	-1	0.1
1	2.3	2.3	2.3	2.7	3.1	3.7
	0.8	0.8	0.9	1	1.1	1.6
	0.2	0.2	0.2	0.3	0.5	1
	-0.6	-0.5	-0.5	-0.3	-0.1	0.6
10	4.6	4.7	4.7	4.9	5.1	6.4
	1.9	1.9	2	2	2.1	2.8
	1.2	1.2	1.2	1.2	1.3	1.8
	0.5	0.5	0.5	0.6	0.6	1.1
100	5.9	5.9	5.9	6	6.1	6.8
	2.5	2.5	2.5	2.6	2.6	3.1
	1.6	1.6	1.6	1.6	1.7	2
	0.9	0.9	0.9	0.9	0.9	1.2
1000	6.4	6.4	6.4	6.5	6.5	6.9
	2.8	2.8	2.8	2.9	2.9	3.1
	1.8	1.8	1.8	1.8	1.8	2
	1	1	1	1	1.1	1.2

Table 7. Percentage error between the averaged numerical and averaged theoretical e_1, for a system with $K1 = 0.01$, $K2 = 1$ and $e = 0$.

$X_0\backslash\ \phi$	0°	90°	180°	270°
10	7.2	17.6	5.3	17.7
20	3.4	7.2	4.5	7.2
30	2.3	4.6	4.4	4.6
50	1.5	2.7	3.4	2.7

Table 8. Orbital elements for the planetary system HD217107, taken by Vogt et al. 2005. The periods are in days, the planetary masses in Jupiter masses and the the semimajor axes in AU. Keep in mind that the planet masses given in the table are not the actual masses, but $M_{planet} \sin i$, where the angle i is the inclination of the orbital plane with the plane of the sky.

Object	Mass	Period	Semimajor axis	Eccentricity
HD217107	$1.053 M_\odot$	—	—	—
HD217107b	$1.37 M_J$	7.1269d	0.074	0.13
HD217107c (Keck)	$2.1 M_J$	3150d	4.3	0.55
HD217107c (Lick)	$3.31 M_J$	2465d	3.6	0.53